

Anisotropy of the quark-antiquark potential in a magnetic field

Claudio Bonati,^{*} Massimo D'Elia,[†] Marco Mariti,[‡] Michele Mesiti,[§] and Francesco Negro[¶]
Dipartimento di Fisica dell'Università di Pisa and INFN - Sezione di Pisa,
Largo Pontecorvo 3, I-56127 Pisa, Italy

Francesco Sanfilippo^{**}
School of physics and astronomy, University of Southampton, SO17 1BJ Southampton, United Kingdom
 (Dated: March 25, 2014)

We investigate the static $\bar{Q}Q$ -potential for $N_f = 2+1$ QCD at the physical point in the presence of a constant and uniform external magnetic field. The potential is found to be anisotropic and steeper in the directions transverse to the magnetic field than in the longitudinal one. In particular, when compared to the standard case with zero background field, the string tension increases (decreases) in the transverse (longitudinal) direction, while the absolute value of the Coulomb coupling and the Sommer parameter show an opposite behavior.

PACS numbers: 12.38.Aw, 11.15.Ha, 12.38.Gc, 12.38.Mh

I. INTRODUCTION

The properties of strong interactions in the presence of a strong magnetic background have attracted much interest in the last few years (see, e.g., Ref. [1] for recent reviews on the subject). This is justified by the many contexts in which such properties may play a role: the physics of compact astrophysical objects, like magnetars [2], of non-central heavy ion collisions [3–6] and of the early Universe [7, 8], involves fields going from 10^{10} Tesla up to 10^{16} Tesla ($|e|B \sim 1 \text{ GeV}^2$).

One important feature is that gluon fields, even if not directly coupled to electromagnetic fields, may undergo significant modifications, through effective QED-QCD interactions induced by quark loop effects [9–16]. Such a possibility has been confirmed by lattice QCD simulations [17–24], resulting in some cases in unexpected behaviors, like inverse magnetic catalysis [19, 24–26].

One of the main attributes of strong interactions is the appearance of a confining potential. In the heavy quark limit, that is related to the expectation value of Wilson loops, so that the confining potential emerges as a property of gauge fields only. It is interesting, then, to ask whether a magnetic background field can influence also the static quark-antiquark potential. Many studies have considered the possible emergence of anisotropies [9, 10, 15, 16], which would be of great phenomenological relevance, leading for instance to modifications in the heavy quark bound states.

Anisotropies in the gauge field distributions have been already observed in quantities like the average plaquette densities taken in different planes [20, 21]. However, a

numerical investigation of the possible anisotropies of the static potential is still missing.

In this paper, we present an exploratory study of this issue, which is based on numerical simulations of $N_f = 2+1$ QCD with physical quark masses, discretized by stout improved staggered fermions and the tree level improved Symanzik pure gauge action. In particular, we will look at the expectation values of Wilson loops in the presence of a magnetic background field, and compute from them the static potential for quark-antiquark separations orthogonal or parallel to the magnetic field direction. We will consider zero temperature, three different lattice spacings and magnetic fields going up to $|e|B \sim 1 \text{ GeV}^2$. Results will show the emergence of significant modifications, which can be parametrized in terms of anisotropies both in the string tension and in the Coulomb part of the potential.

II. NUMERICAL METHODS

We have considered $N_f = 2+1$ QCD in the presence of a constant and uniform magnetic field, which enters the QCD Lagrangian through quark covariant derivatives $D_\mu = \partial_\mu + igA_\mu^a T^a + iq_f A_\mu$, where A_μ is the abelian gauge potential and q_f is the quark electric charge. On the lattice, that amounts to adding proper $U(1)$ phases to the usual $SU(3)$ links entering the Dirac operator. The Euclidean partition function is expressed as

$$\mathcal{Z}(B) = \int \mathcal{D}U e^{-S_{YM}} \prod_{f=u,d,s} \det(D_{st}^f[B])^{1/4}, \quad (1)$$

$$S_{YM} = - \sum_i \frac{\beta}{3} \left(\sum_{\mu\nu} c_0 W_{i;\mu\nu}^{1 \times 1} + c_1 W_{i;\mu\nu}^{1 \times 2} \right), \quad (2)$$

^{*}Electronic address: bonati@df.unipi.it

[†]Electronic address: delia@df.unipi.it

[‡]Electronic address: mariti@df.unipi.it

[§]Electronic address: mesiti@df.unipi.it

[¶]Electronic address: fnegro@pi.infn.it

^{**}Electronic address: f.sanfilippo@soton.ac.uk

$$(D_{\text{st}}^f)_{i,j} = am_f \delta_{i,j} + \sum_{\nu=1}^4 \frac{\eta_{i;\nu}}{2} \left(u_{i;\nu}^f U_{i;\nu}^{(2)} \delta_{i,j-\hat{\nu}} - u_{i-\hat{\nu};\nu}^{f*} U_{i-\hat{\nu};\nu}^{(2)\dagger} \delta_{i,j+\hat{\nu}} \right) \quad (3)$$

where \mathcal{DU} is the functional integration over the non-abelian $SU(3)$ gauge link variables. \mathcal{S}_{YM} is the tree level improved Symanzik action [29, 30], which involves the real part of the trace of the 1×1 ($W_{i;\mu\nu}^{1 \times 1}$) and 1×2 ($W_{i;\mu\nu}^{1 \times 2}$) loops, with coefficients $c_0 = 5/3$ and $c_1 = -1/12$.

D_{st}^f is the staggered Dirac operator, built up in terms of two times stout-smear links $U_{i;\mu}^{(2)}$ [31] (with isotropic smearing parameters $\rho_{\mu\nu} = 0.15 \delta_{\mu\nu}$), in order to reduce finite cut-off effects and, in particular, taste symmetry violations.

As for the electromagnetic degrees of freedom, the continuum gauge potential $A_y = Bx$ and $A_\mu = 0$ for $\mu = t, x, z$, corresponding to a magnetic field in the \hat{z} direction, is discretized on the lattice torus as follows

$$u_{i;y}^f = e^{ia^2 q_f B i_x}, \quad (4)$$

$$u_{i;x}^f|_{i_x=L_x} = e^{-ia^2 q_f L_x B i_y} \quad (5)$$

with $u_{i;\mu}^f = 1$ elsewhere and B quantized as [32–35]

$$|e|B = 6\pi b / (a^2 L_x L_y), \quad (6)$$

where b is an integer. No stout smearing is applied to the $U(1)$ phases, which are treated as purely external parameters (quenched QED approximation).

We have performed simulations at the physical value of the pion mass, $m_\pi \sim 135$ MeV, using the bare parameters β , $am_{u,d}$ and am_s ($m_s/m_{u,d}$ is fixed to its physical value, 28.15) reported in Table I, which correspond to a line of constant physics at three different values of the lattice spacing a . We have explored symmetric, zero temperature lattices, with the number of sites per direction (L) chosen so as to maintain an extent around 5 fm for all values of a . The Rational Hybrid Monte-Carlo (RHMC) algorithm has been used for the sampling of gauge configurations, with statistics ranging, for each value of B , from $O(10^4)$ to $O(10^3)$ molecular dynamics (MD) time units, going from the coarsest to the finest lattice.

In order to determine the spin-averaged potential between a static $\bar{Q}Q$ pair, separated by a distance \vec{R} , we have considered the large time behavior of the average

L	$a(\text{fm})$	β	$am_{u/d}$	am_s	b
24	0.2173(4)	3.55	0.003636	0.1020	0,12,16,24,32,40
32	0.1535(3)	3.67	0.002270	0.0639	0,12,16,24,32,40
40	0.1249(3)	3.75	0.001787	0.0503	0,8,12,16,24,32,40

TABLE I: Simulation parameters: the bare coupling β and the quark masses $am_{u/d}$ and am_s are chosen following Refs. [27, 28], corresponding to a physical pion mass. The errors reported are just the statistical ones, the systematic error is about 2% (see the discussion in Ref. [27]).

rectangular Wilson loop $W(\vec{R}, T)$, where T indicates the time extension of the loop. Usually, based on space-time isotropy, one averages over all directions of \vec{R} ; on the contrary, apart from the $B = 0$ case, we will consider separately the averages over different directions, thus leaving room to the possibility that $V(\vec{R})$ may not be a central potential.

In particular, going to a lattice notation, in which \vec{n} and n_t denote the dimensionless spatial and temporal sides of the loop, the potential can be obtained as

$$aV(a\vec{n}) = \lim_{n_t \rightarrow \infty} \log \left(\frac{\langle W(a\vec{n}, a n_t) \rangle}{\langle W(a\vec{n}, a(n_t + 1)) \rangle} \right). \quad (7)$$

In practice, one plots the right-hand side as a function of n_t and looks for a stable plateau at large times, from which the potential can be extracted by a suitable fit to a constant function. In the present study we will limit ourselves to the cases of \vec{n} parallel or orthogonal to \vec{B} , which will be denoted respectively by Z and XY (average over orthogonal directions).

For each simulation, we have measured Wilson loops every 5 MD time units. In order to reduce the UV noise, we have applied one single step of HYP smearing [36] for temporal links, adopting the same smearing parameters as in Ref. [37], corresponding to the so-called HYP2-action, and N_{SM} steps of APE-smearing [38] for spatial links, with smearing parameter $\alpha_{\text{APE}} = 0.25$.

Since APE-smearing treats all spatial directions symmetrically, it is important to check that possible anisotropies be not washed out by this noise reduction technique. We have studied, for a few cases, the dependence of results on the number of smearing steps and, having checked that it is not significant (see next section), we have fixed $N_{SM} = 24$. The statistical errors on the right-hand side of Eq. (7), as well as those on the parameters of the fitted plateaux, have been determined by performing a bootstrap analysis, in order to take correlations into account.

III. NUMERICAL RESULTS

In Fig. 1 we report an example of the logarithm of Wilson loop ratios, see Eq. (7), as a function of n_t and for different APE-smearing levels, obtained at spatial distance $|\vec{n}| = 3$ and for $|e|B = 0.97 \text{ GeV}^2$. We show separately results averaged over the longitudinal (Z) or transverse (XY) directions. A well defined plateau is visible in both cases, and the emergence of an anisotropy already clearly appears, with the potential being larger in the transverse direction. It is also evident that smearing has no visible effect on such anisotropy, so that one can safely adopt a number of smearing levels large enough to have a good noise/signal ratio.

In Fig. 2 we report an example of the potential, as a function of the $\bar{Q}Q$ separation, determined for our smallest lattice spacing and for two values of the magnetic

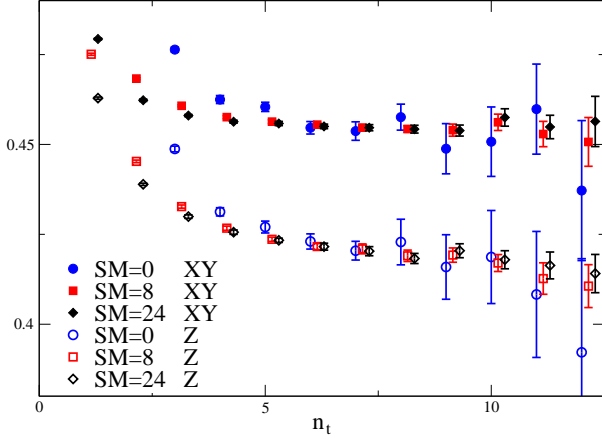


FIG. 1: Wilson loop combination defined in Eq. 7 for $|\vec{n}| = 3$ as a function of n_t and for several values of the APE smearing level. The simulation was performed on the 32^4 lattice at $|e|B = 0.97 \text{ GeV}^2$.

field, $eB = 0$ and $eB \simeq 0.7 \text{ GeV}^2$ ($b = 24$). In the former case we have averaged over all spatial directions. For $B \neq 0$ we observe a clear anisotropic behavior, with a striking separation of the values of the potential measured along the Z or XY directions. A comparison with $B = 0$ shows that the potential increases in the transverse directions and decreases in the longitudinal direction. This behavior has been observed for all the explored lattice spacings, starting from magnetic fields of the order $eB \simeq 0.2 \text{ GeV}^2$.

In the same figure we also show, for $B \neq 0$, the potential obtained by averaging Wilson loops over all spatial directions (denoted by XYZ). It is interesting to notice that in this case the effect of B on the static potential is strongly reduced. This fact may explain why previous studies have not observed significant effects of the external field on the static potential [19].

In order to better characterize the dependence of the potential on the magnetic field, we have fitted it, for each value of B and for transverse and longitudinal directions separately, according to the standard Cornell parametrization:

$$aV(a\hat{d}) = \hat{c}_d + \hat{\sigma}_d n + \frac{\alpha_d}{n}, \quad (8)$$

where \hat{d} is a unit vector taken either along the z or along xy directions, $\hat{\sigma}_d$ is the string tension, α_d the Coulomb coupling, \hat{c}_d a constant term, and the suffix d is there to take into account the possible dependence on the direction. Such a parametrization fits reasonably well the measured potentials, with the $\chi^2/\text{d.o.f.}$ parameter around 1 or below for all the explored fields and in a distance range going from ~ 0.3 to $\sim 1 \text{ fm}$. In our fits we have set $\alpha_d = \hat{r}_{0d}^2 \hat{\sigma}_d - 1.65$, in order to determine the string tension and the Sommer parameter \hat{r}_{0d} as independent quantities. A bootstrap analysis has been performed to determine the best fit parameters and their statistical errors.

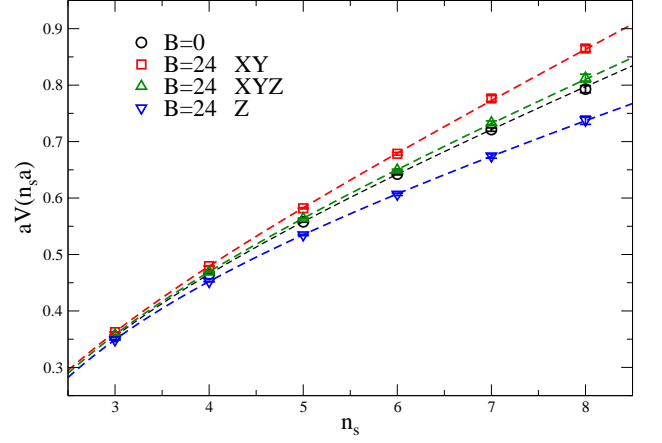


FIG. 2: $\bar{Q}Q$ -potential both for $|e|B = 0$ and for $|e|B = 0.7 \text{ GeV}^2$ on the 40^4 lattice.

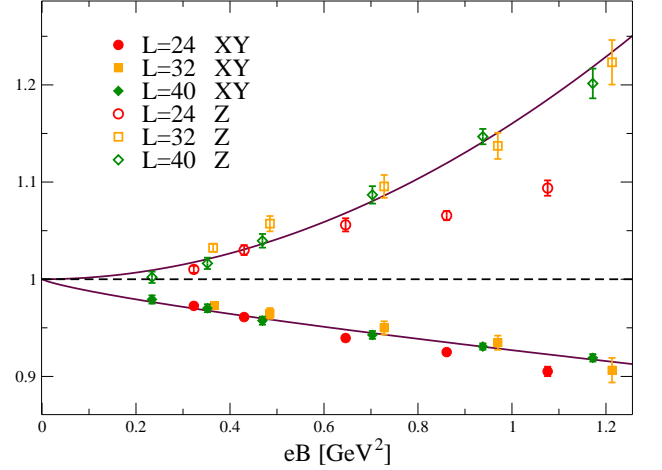


FIG. 3: Plot of R^{r0} along the directions Z and XY. The solid line is the fit according to Eq. (10) for the $L = 40$ data: we obtained $A^{r0xy} = -0.0729(2)$, $C^{r0xy} = 0.78(6)$ with $\chi^2/\text{dof} = 0.49$ and $A^{r0z} = 0.160(6)$, $C^{r0z} = 1.9(1)$ with $\chi^2/\text{dof} = 1.33$.

In order to better monitor the dependence of the fitted parameters on B , we have normalized them to the values they take for $B = 0$ at the same lattice spacing, i.e. we have determined the quantities

$$R^{\mathcal{O}_d} = \frac{\mathcal{O}_d(|e|B)}{\mathcal{O}_d(|e|B = 0)}, \quad (9)$$

which are shown in Figs. 3, 4 and 5, respectively for $\mathcal{O}_d = \hat{\sigma}_d$, \hat{r}_{0d} and α_d .

The observed anisotropy in the potential reflects in these quantities, leading to a significant splitting of the corresponding ratios, which are of the order of 10–20%. In particular, the string tension increases (decreases), as a function of eB , in the trasverse (longitudinal) direction, while the parameter \hat{r}_0 and the Coulomb coupling show an opposite behavior.

Our results show a mild dependence on the lattice spacing, apart from the largest fields on the coarsest lattice,

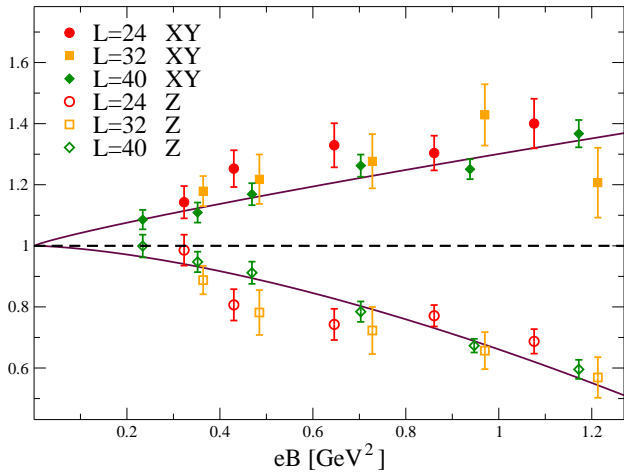


FIG. 4: Plot of R^σ along the Z and XY directions. The solid line is the fit according to Eq. (10) for the $L = 40$ data: we obtained $A^{r_{0xy}} = 0.30(2)$, $C^{r_{0xy}} = 0.8(1)$ with $\chi^2/\text{dof} = 1.00$ and $A^{r_{0z}} = -0.33(1)$, $C^{r_{0z}} = 1.5(2)$ with $\chi^2/\text{dof} = 0.96$.

for which $eB \sim 1/a^2$; however the present accuracy of our data does not permit a proper continuum extrapolation. We have fitted the $L = 40$ data (i.e. corresponding to our finest lattice spacing) according to the following ansatz for the dependence of each ratio on B :

$$R^{\mathcal{O}_d} = 1 + A^{\mathcal{O}_d} (|e|B)^{C^{\mathcal{O}_d}}; \quad (10)$$

the best fit results are shown as continuous lines in the figures.

IV. DISCUSSION AND CONCLUSIONS

The weak dependence of our data on a suggests that what we have observed is a genuine continuum phenomenon. However, it is important to exclude other exotic possibilities, like for instance a non-trivial, anisotropic dependence of the lattice spacing on B . In particular, an increase of a_z and a decrease of a_{xy} as a function of B would lead to similar observations. In fact, the magnetic field in the \hat{z} direction breaks the original $SO(4)$ symmetry of the Euclidean theory down to a $SO(2)_{xy} \times SO(2)_{zt}$ symmetry. A possible effect, in the lattice regularized theory, could be an anisotropy in the lattice spacings, which however should still respect $a_z = a_t$ and $a_x = a_y$.

An investigation of the dependence of the lattice spacing on B has been reported in Ref. [19], leading to the conclusion that the dependence is not significant. Part of the evidence, which is based on the analysis of r_0 , is not useful, in view of the fact that we observe an anisotropy for this parameter. However, the dependence of the charged pion mass on eB , which is reported in Fig. 1-left of Ref. [19] and involves both a_t (to get the physical value of the pion mass) and a_{xy} (to get the physical value of eB) clearly shows that such a non-trivial de-

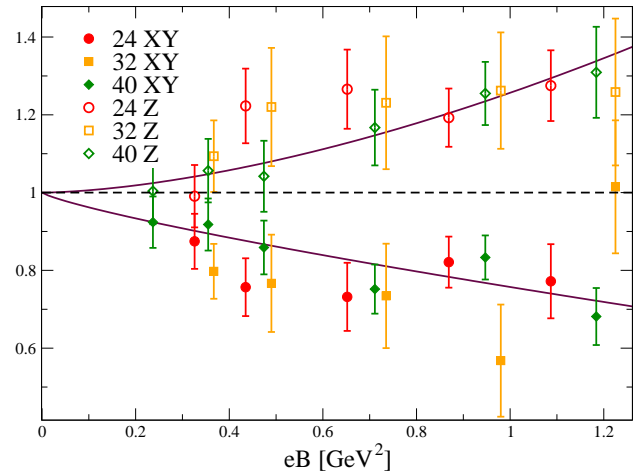


FIG. 5: Plot of R^α along the Z and XY directions. The solid line is the fit according to Eq. (10) for the $L = 40$ data: we obtained $A^{\alpha_{xy}} = -0.24(3)$, $C^{\alpha_{xy}} = 0.7(4)$ with $\chi^2/\text{dof} = 0.93$ and $A^{\alpha_z} = 0.24(5)$, $C^{\alpha_z} = 1.8(9)$ with $\chi^2/\text{dof} = 0.14$.

pendence is not present, at least for eB up to $\sim 0.4 \text{ GeV}^2$. On the other hand, at such field values, the anisotropies that we observe in the static potential are already clearly visible.

Regarding the physical origin of the observed anisotropy, it is clear that it is induced by the effective couplings between electromagnetic and chromoelectric - chromomagnetic fields, which take origin from quark loop contributions. At the perturbative level [21] the effective action predicts an increase of the chromoelectric field components orthogonal to \vec{B} (see also Ref. [15]), and a suppression of the longitudinal one; such a prediction is also in agreement with the observed anisotropies at the plaquette level [20, 21]. Since confinement is related to the formation of a chromoelectric flux-tube, this result suggests an increase (decrease) of the string tension in the direction trasverse (parallel) to \vec{B} , as we have found. Possible anisotropies in the static potential have been predicted also in Ref. [9], in particular a decrease of the Coulomb coupling in the transverse direction, which is consistent with our observations.

Our exploratory study claims for future investigations in various directions. While in this context we have limited ourselves to the computation of the potential in the Z and XY directions, next studies will have to map the complete form of the potential, in particular to understand its dependence on the angle ϕ with respect to the magnetic field direction. On general grounds, this dependence is expected to be even in $\cos \phi$ (by charge conjugation invariance). Another interesting feature of the modifications in the potential, which should be better understood in the future, is the fact that they get largely suppressed when one averages Wilson loops over all spatial directions. A detailed study of the flux tube profile for the various directions will be necessary to get a clear picture about B -dependent modifications of the chromo-

electric fields.

Another direction for future studies is related to the possible phenomenological consequences of our findings. To that aim, it will be necessary to extend the investigation to finite temperature, in order to have predictions valid also in the context of non-central heavy ion collisions. The spectrum of mesons in the presence of a strong magnetic background has attracted much interest in the recent past [39–42], and will likely get significant corrections by the presence of anisotropies in the quark-antiquark potential; along this direction, a lattice measurement of heavy quark bound states in the presence of a magnetic background will be of great importance. Finally, the fact that quarks experience a different attractive force when they try to separate in the direction parallel or orthogonal to the magnetic field, may have

consequences on various experimental probes, like for instance the elliptic flow.

Acknowledgments

We thank M. Chernodub and E. Laermann for useful discussions. FS thanks Michael Kruse for useful discussions regarding code optimization on the Blue Gene/Q machine. FN acknowledges financial support from the EU under project Hadron Physics 3 (Grant Agreement n. 283286). Numerical simulations have been performed on the Blue Gene/Q Fermi machine at CINECA, based on the agreement between INFN and CINECA (under INFN projects PI12 and NPQCD).

-
- [1] D. Kharzeev, K. Landsteiner, A. Schmitt and H. -U. Yee, Lect. Notes Phys. **871**, 1 (2013).
 - [2] R. C. Duncan and C. Thompson, Astrophys. J. **392**, L9 (1992).
 - [3] V. Skokov, A. Y. Illarionov and V. Toneev, Int. J. Mod. Phys. A **24**, 5925 (2009) [arXiv:0907.1396 [nucl-th]].
 - [4] V. Voronyuk, V. D. Toneev, W. Cassing, E. L. Bratkovskaya, V. P. Konchakovski and S. A. Voloshin, Phys. Rev. C **83**, 054911 (2011) [arXiv:1103.4239 [nucl-th]].
 - [5] A. Bzdak and V. Skokov, Phys. Lett. B **710**, 171 (2012) [arXiv:1111.1949 [hep-ph]].
 - [6] W. -T. Deng and X. -G. Huang, Phys. Rev. C **85**, 044907 (2012) [arXiv:1201.5108 [nucl-th]].
 - [7] T. Vachaspati, Phys. Lett. B **265**, 258 (1991).
 - [8] D. Grasso and H. R. Rubinstein, Phys. Rept. **348**, 163 (2001) [astro-ph/0009061].
 - [9] V. A. Miransky and I. A. Shovkovy, Phys. Rev. D **66**, 045006 (2002);
 - [10] M. N. Chernodub, arXiv:1001.0570 [hep-ph].
 - [11] M. M. Musakhanov and F. C. Khanna, hep-ph/9605232.
 - [12] H. T. Elze and J. Rafelski, In *Sandansky 1998, Frontier tests of QED and physics of the vacuum* 425-439 [hep-ph/9806389].
 - [13] H. T. Elze, B. Muller and J. Rafelski, hep-ph/9811372.
 - [14] M. Asakawa, A. Majumder and B. Muller, Phys. Rev. C **81**, 064912 (2010).
 - [15] B. V. Galilo and S. N. Nedelko, Phys. Rev. D **84**, 094017 (2011).
 - [16] S. Ozaki, arXiv:1311.3137 [hep-ph].
 - [17] M. D’Elia, S. Mukherjee and F. Sanfilippo, Phys. Rev. D **82**, 051501 (2010) [arXiv:1005.5365 [hep-lat]].
 - [18] M. D’Elia and F. Negro, Phys. Rev. D **83**, 114028 (2011) [arXiv:1103.2080 [hep-lat]].
 - [19] G. S. Bali, F. Bruckmann, G. Endrodi, Z. Fodor, S. D. Katz, S. Krieg, A. Schafer and K. K. Szabo, JHEP **1202**, 044 (2012) [arXiv:1111.4956 [hep-lat]].
 - [20] E. -M. Ilgenfritz, M. Kalinowski, M. Muller-Preussker, B. Petersson and A. Schreiber, Phys. Rev. D **85**, 114504 (2012) [arXiv:1203.3360 [hep-lat]].
 - [21] G. S. Bali, F. Bruckmann, G. Endrodi, F. Gruber and A. Schaefer, JHEP **1304**, 130 (2013) [arXiv:1303.1328 [hep-lat]].
 - [22] M. D’Elia, M. Mariti and F. Negro, Phys. Rev. Lett. **110**, 082002 (2013) [arXiv:1209.0722 [hep-lat]].
 - [23] F. Bruckmann, G. Endrodi and T. G. Kovacs, JHEP **1304**, 112 (2013) [arXiv:1303.3972 [hep-lat]].
 - [24] E. -M. Ilgenfritz, M. Muller-Preussker, B. Petersson and A. Schreiber, arXiv:1310.7876 [hep-lat].
 - [25] I. A. Shovkovy, Lect. Notes Phys. **871**, 13 (2013) [arXiv:1207.5081 [hep-ph]].
 - [26] K. Fukushima and Y. Hidaka, Phys. Rev. Lett. **110**, 031601 (2013) [arXiv:1209.1319 [hep-ph]].
 - [27] Y. Aoki, S. Borsanyi, S. Durr, Z. Fodor, S. D. Katz, S. Krieg and K. K. Szabo, JHEP **0906**, 088 (2009) [arXiv:0903.4155 [hep-lat]].
 - [28] S. Borsanyi, G. Endrodi, Z. Fodor, A. Jakovac, S. D. Katz, S. Krieg, C. Ratti and K. K. Szabo, JHEP **1011**, 077 (2010) [arXiv:1007.2580 [hep-lat]].
 - [29] P. Weisz, Nucl. Phys. B **212**, 1 (1983).
 - [30] G. Curci, P. Menotti and G. Paffuti, Phys. Lett. B **130**, 205 (1983) [Erratum-ibid. B **135**, 516 (1984)].
 - [31] C. Morningstar and M. J. Peardon, Phys. Rev. D **69**, 054501 (2004) [hep-lat/0311018].
 - [32] G. ’t Hooft, Nucl. Phys. B **153**, 141 (1979).
 - [33] P. H. Damgaard and U. M. Heller, Nucl. Phys. B **309**, 625 (1988).
 - [34] M. H. Al-Hashimi and U. J. Wiese, Ann. Phys. **324**, 343 (2009) [arXiv:0807.0630 [quant-ph]].
 - [35] M. D’Elia, Lect. Notes Phys. **871**, 181 (2013) [arXiv:1209.0374 [hep-lat]].
 - [36] A. Hasenfratz and F. Knechtli, Phys. Rev. D **64**, 034504 (2001) [hep-lat/0103029].
 - [37] M. Della Morte, A. Shindler and R. Sommer, JHEP **0508**, 051 (2005) [hep-lat/0506008].
 - [38] M. Albanese *et al.* [APE Collaboration], Phys. Lett. B **192** (1987) 163.
 - [39] M. N. Chernodub, Phys. Rev. Lett. **106**, 142003 (2011) [arXiv:1101.0117 [hep-ph]].
 - [40] Y. Hidaka and A. Yamamoto, Phys. Rev. D **87**, 094502 (2013) [arXiv:1209.0007 [hep-ph]].
 - [41] M. A. Andreichikov, B. O. Kerbikov, V. D. Orlovsky and Y. A. Simonov, Phys. Rev. D **87**, 094029 (2013) [arXiv:1304.2533 [hep-ph]].

- [42] J. Alford and M. Strickland, Phys. Rev. D **88**, 105017 (2013) [arXiv:1309.3003 [hep-ph]].